New Paradigm for the Isotope Scaling of Plasma Transport Paradox

V. Sokolov and A. K. Sen
Plasma Physics Laboratory, Columbia University, New York, New York 10027, USA
(Received 21 August 2003; published 20 April 2004)

Most tokamak experimental results [M. Bessenrodt-Weberpals *et al.*, Nucl. Fusion **33**, 1205 (1993)] and basic physics experiments [V. Sokolov and A. K. Sen, Phys. Rev. Lett. **89**, 095001 (2002)] in the Columbia Linear Machine indicate dependence of the ion thermal conductivity on the isotopic mass close to $\chi_\perp \sim A_i^{-0.5}$, i.e., inverse gyro-Bohm. This is in stark contradiction to most present theoretical models predicting Bohm (A_i^0) or gyro-Bohm ($A_i^{0.5}$) scaling. A series of experiments designed to explore the physics basis of this scaling appears to lead to a new model for this scaling based on 3-wave coupling of two ion temperature gradient radial harmonics and an ion acoustic wave.

DOI: 10.1103/PhysRevLett.92.165002 PACS numbers: 52.35.Kt, 52.35.Mw

Isotope scaling of particle and heat transport is an important issue for magnetic fusion as well as basic plasma physics. As there is wide divergence between most theoretical predictions and tokamak experimental results, this has become a fundamental open physics issue of great importance. All Bohm-like scaling of transport parameters indicate $D_\perp, \chi_\perp \sim A_i^0$, while gyro-Bohm-like scaling implies $\sim A_i^{0.5}$, where A_i is the mass number of the isotope of hydrogen. These include most of the latest results of ion temperature gradient (ITG) turbulence, resistive ballooning mode theories, as well as 2D and 3D gyrofluid and gyrokinetic simulations. However, the Bohm or gyro-Bohm-like scaling is in stark contrast with the vast majority of tokamak experiments $D_\perp, \chi_\perp \sim A_i^{-0.5}$ [1].

We now summarize a few relevant theories, which attempt to explain the puzzling inverse gyro-Bohm scaling. Coppi [2] derives a scaling $A_i^{-2/5}$ that is close to the experimental results, based on impurity species response to ITG modes. This mechanism is not applicable in the Columbia Linear Machine (CLM), where the impurity levels are truly negligible. Scott [3] has a theory based on nonlinear excitation of dissipative drift waves, which leads to a scaling similar to the experimental results. However, this theory is not appropriate for the collisionless plasma in both the core of tokamaks and the CLM. In fact, the collisionality in CLM is very low as $\nu_{e,i}^* \sim 10^{-2}$, where ν^* is the collision frequency normalized to bounce or transit frequency of the particles. The most interesting and plausible mechanism proposed by Waltz [4] and Ernst [5] is based on $\mathbf{E} \times \mathbf{B}$ and diamagnetic flow shear, which leads to the breaking of gyro-Bohm scaling. But in the CLM the $\mathbf{E} \times \mathbf{B}$ and diamagnetic flow shears are identical for two gases, as mentioned below and reported before [6]. Last, the 3D gyrokinetic code results of Lee and Santoro [7], interpreted in terms of Dupree's resonance broadening decorrelation concept [8], predict an inverse gyro-Bohm scaling of transport $\sim A_i^{-0.5}$. This is a very interesting basic physics perspective. Unfortunately, their critical result indicating higher spectral amplitudes and widths for lower isotopic mass are in contradiction with CLM results, where these are nearly identical as described below and reported earlier [6].

We start by considering the following causal chain for transport due to ITG modes: linear instability drive $(\gamma) \rightarrow$ saturated fluctuation level n established via nonlinear turbulent dynamics $\rightarrow$ statistical mechanics of scattering of energy by turbulence leading to a transport parameter $\chi_\perp$. In our previous experiments [6] we obtained isotope scaling $\chi_\perp \sim A_i^{-0.5}$ for the same $\tilde{n}/n_0$, and $\chi_\perp \sim A_i^{-0.65-0.85}$ for the same η_i over a broad set of discharges. For the set of experiments with nearly identical profiles of all plasma parameter profiles we reported the result $\chi_\perp \sim A_i^{-0.5}$. We particularly refer to this result in the following pages. The present research continues the investigation of each step of this causal chain.

The layout of the CLM has been described in Ref. [9]. Gated feedback [10] as shown in Fig. 1 is used as a diagnostic technique to measure the linear growth rate of the ITG instability. The mode is first stabilized nearly to noise level, and then the feedback circuit is electronically opened in μsec time scale, allowing the free growth of the instability and subsequent nonlinear saturation. It

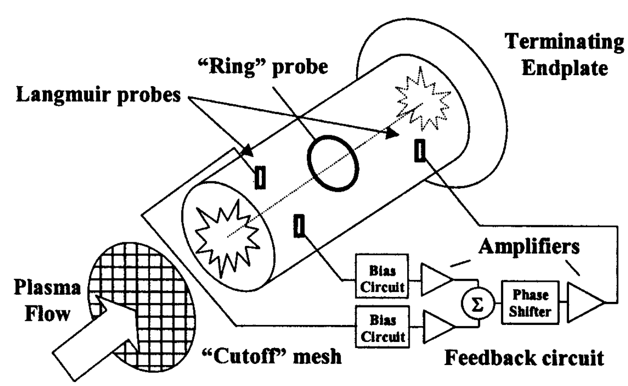

FIG. 1. Layout of several diagnostics in the Columbia Linear Machine.

is noted that two probes placed at opposite locations in azimuth (0° and 180°) are connected as a spatial filter for the elimination of odd azimuthal modes, in particular, the $m = 1$ rotational flute mode [11], which is always present in the CLM. The typical data, averaged over 500 shots, used the Van der Pol equation for fitting the data to yield a growth rate γ. The resulting Fig. 2 reveals an isotopic effect $\gamma \sim \tilde{n}/n_0, A_i^{-0.3}$. Linear theories of slab ITG modes reveal only a weak isotopic dependence γ (slab ITG) $\sim (k_{\text{II}}^2 C_S^2 \omega_T^*)^{1/3} \sim A_i^{-1/3}$ [12], which is remarkably similar to our experiment. Parenthetically, the linear growth rate of toroidal ITG modes have no isotopic dependence for a fixed k_y, but its maximum obtained at $k_y \rho_i \sim$ const (≤ 1) scales as $\gamma_{\max} \sim A_i^{-1/2}$, where k_y and ρ_i are the wave number in the diamagnetic drift direction and gyroradius, respectively [12]. Finally, this weak isotopic dependence in CLM is far from sufficient to explain the inverse gyro-Bohm scaling of transport.

The effects of flow (transverse to magnetic field) shear are important for the suppression of instabilities and transport, which potentially can be mass dependent. In our previous study [6], we were able to maintain the plasma potential profile $\Phi(r)$ to be nearly identical for both gases, thus ensuring identical radial electric field and azimuthal (poloidal) flow profile and its shear. However, parallel (to the magnetic field) flow shear has a destabilizing effect (Kelvin-Helmholtz drive) [13], which can potentially have an isotopic effect. Therefore, we carefully study this possibility via measurements of the radial profiles of parallel velocity for both gases, which are observed to be identical, indicating no mass dependence. Therefore, we can conclude that no isotopic effects on plasma transport in the CLM are attributable to the linear (as well as nonlinear) dynamical features of flow shear—either stabilizing or destabilizing.

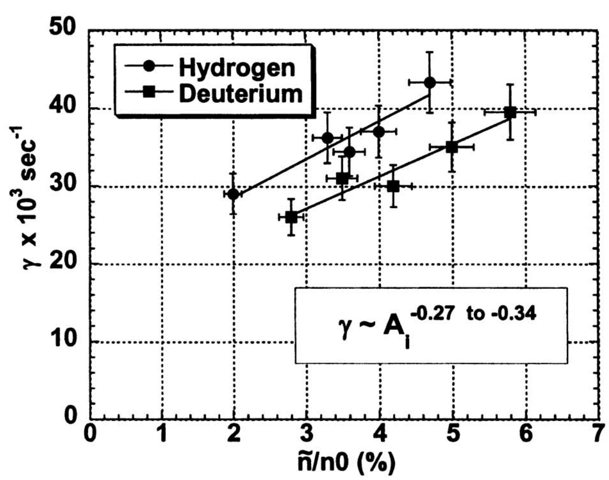

FIG. 2. Linear growth rate as a function of $\tilde{n}/n_0$ for both gases.

We now turn to the isotopic effects at the nonlinear dynamics level. Specifically, we investigate the possibility of 3-wave coupling [12], which has been proved to be useful in many cases and is defined by the following resonance conditions:

$$\omega_1 \pm \omega_2 = \omega_3, \qquad \mathbf{k}_1 \pm \mathbf{k}_2 = \mathbf{k}_3, \tag{1}$$

where $\omega_i = \omega_i(\mathbf{k}_i)$ is the dispersion relation of ITG modes.

It is noted that in the CLM the mode frequency is Doppler shifted by the equilibrium $\mathbf{E}_0 \times \mathbf{B}_0$ rotation of the plasma column with frequency $\omega_E = (m/r)\mathbf{E}_0 \times \mathbf{B}_0$, where m is the azimuthal mode number. Then the Doppler shift frequency ω_E also obeys the selection rule of 3-wave resonant mode coupling:

$$m_1(\mathbf{k}_1) \pm m_2(\mathbf{k}_2) = m_3(\mathbf{k}_3), \qquad \omega_{E1} \pm \omega_{E2} = \omega_{E3}. \tag{2}$$

The presence of 3-wave coupling is easily revealed in the bispectrum [14]. The normalized autobispectrum, called the autobicoherency, is defined as

$$b^2(\omega_1, \omega_2) = \frac{|\langle X(\omega_1)X(\omega_2)X^*(\omega_1 + \omega_2)\rangle|^2}{\langle |X(\omega_1)X(\omega_2)|^2\rangle\langle |X(\omega_1 + \omega_2)|^2\rangle},$$

where $X(\omega_i)$ are Fourier amplitudes.

The fast Fourier transform algorithm was used to generate the Fourier transforms of each of the 512 samples ($dt = 1$ μsec, 1024 points). The frequency resolution is $\Delta f = 1$ kHz, and the variance (noise floor) of the bicoherence can be estimated as $db^2(\omega_1, \omega_2) \leq 1/N \sim 0.002$, where N equals the number of samples. Figure 3(a) shows a typical bicoherence and corresponding power spectrum. The *X*, *Y* coordinates are ω_1 and ω_2 in the figure, and the third frequency and wave number follow from the resonance condition of Eq. (1). It is noted that there are no significant explicit differences between the bispectra for two gases. Similarly there is no substantive difference in the power spectra for the two gases [6].

We now propose a radically new paradigm for the isotope scaling conundrum. We have shown that no significant isotopic effect is apparent in the nonlinear dynamical level, as revealed by bispectral analysis. This prompts a closer examination of the detailed maps of the bicoherence and their implications, as shown in Fig. 3, especially for a search for coupling to ion acoustic modes that can provide an ion mass dependent damping. The magnitude of bicoherence is indicated by the grey scale in Fig. 3(a), along with the power spectrum for interpretation. The same is shown in Fig. 3(b) by density of contours of constant bicoherence over a different scale. Here the dense patches on the diagonal ($\omega_1 = \omega_2$) indicate self-coupling and off-diagonal patches indicate cross coupling. The bicoherence corresponding to cross coupling between the ITG mode ω_1 and the low frequency $\omega_2 < 2\pi \times 15$ kHz mode is seen in Fig. 3(a) as a vertical

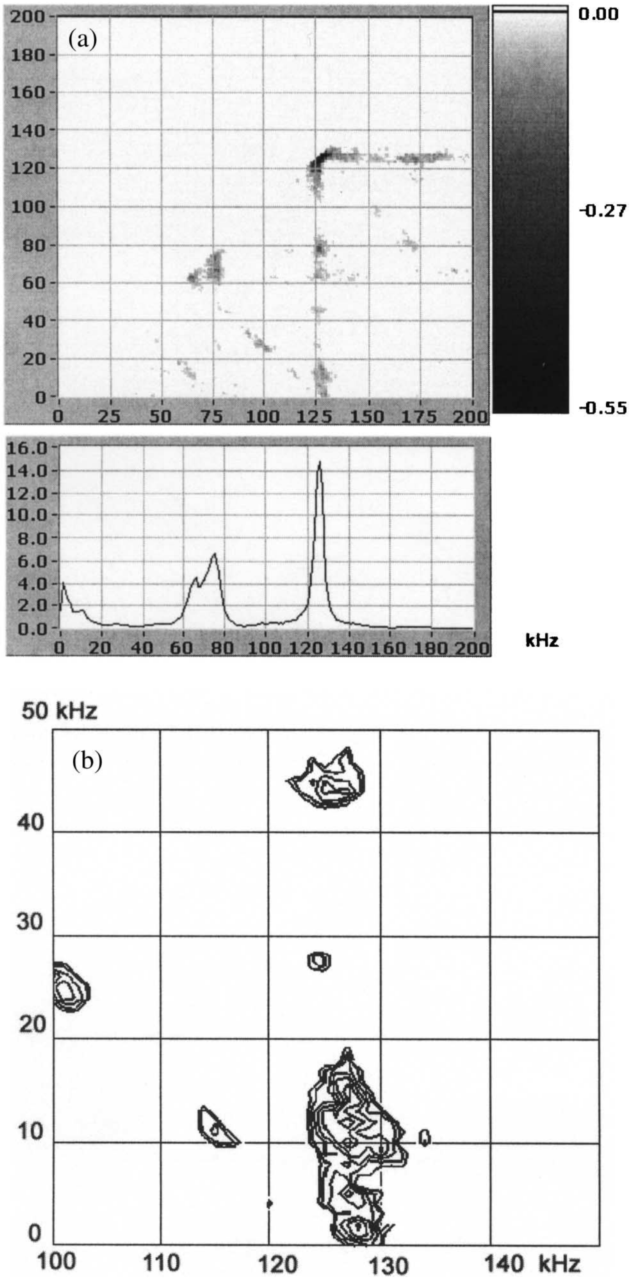

FIG. 3. The bicoherence of ITG mode coupling: (a) bicoherence and corresponding power spectrum; (b) a close-up of the bicoherence.

patch and as dense vertical contours in Fig. 3(b). This may indicate mode coupling between one low frequency mode $\omega_2 \sim 2\pi \times (5\text{–}15)$ kHz (which is visible in the low frequency end of the power spectrum) and two radial harmonics, $\omega_1 = \omega_{20}$ $(m = 2, l = 0)$, $\omega_3 = \omega_{21}$ $(m = 2, l = 1)$ (not visible in the bicoherence), of ITG modes, where m, l refer to azimuthal and radial harmonic mode numbers, respectively. Last, the corresponding wave number matching condition for 3-wave coupling $(m_1 = 2) + (m_2 = 0) \Rightarrow (m_3 = 2)$ indicates a plane wave (without azimuthal structure) nature of the low frequency wave of the triad. It remains to identify the low frequency mode at 5–15 kHz of the triad and confirm its $m_2 = 0$ nature as shown below.

It can be shown that the fluid nonlocal eigenmode equation [15] for the case of nonuniform temperature gradient profiles yields two radial harmonics ω_{20} $(m = 2, l = 0)$ and ω_{21} $(m = 2, l = 1)$, whose difference $\Delta\omega = \omega_{21} - \omega_{20} \sim 2\pi(5\text{–}10)$ kHz for CLM parameters, which is close to the frequency ω_2 of the triad.

We now discuss the clear identification of the low frequency (ω_2) mode of the triad discussed above. Its azimuthal mode number is determined from the azimuthal phase shift measured via cross correlation of two Langmuir probes, displaced azimuthally 90° (180°) apart to yield $m_2 = 0$. Next the parallel wavelength is determined from the axial phase shift measured via cross correlation of two Langmuir probes, displaced axially by 33 cm. The resulting phase shift shown in Fig. 4 indicates that at low frequencies $\omega_2/2\pi < 15$ kHz, it is a linear function of frequency. The reciprocal of the slope of this line yields a phase velocity that is in very good agreement with acoustic wave speed $C_s \sim 6 \times 10^6$ cm/sec calculated for CLM parameters (for hydrogen plasma). Furthermore, this wave speed is found to be different for the two gases by a factor of $\sqrt{2}$, which is another definitive confirmation of the identification of the ion acoustic (IA) mode. Therefore, the low frequency mode in the triad is definitively a plane ion acoustic mode with $m_2 = 0$ and $\omega_2/2\pi < 15$ kHz. Last, it is not a zonal flow, because $k_{\parallel} \neq 0$ in this case.

We now present another experimental evidence of coupling between ITG modes and the IA mode (besides the bicoherence data). This evidence is based on probing the coupling via feedback diagnostic, which is unique in CLM. We use the feedback described before to destabilize the ITG mode $(m = 2)$ and enhance its amplitude and observe its effects on the IA mode amplitude. To enhance

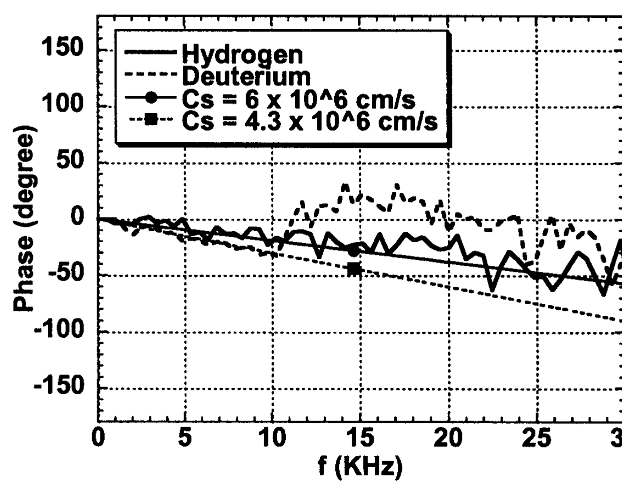

FIG. 4. Ion acoustic velocity C_s from axial phase shift.

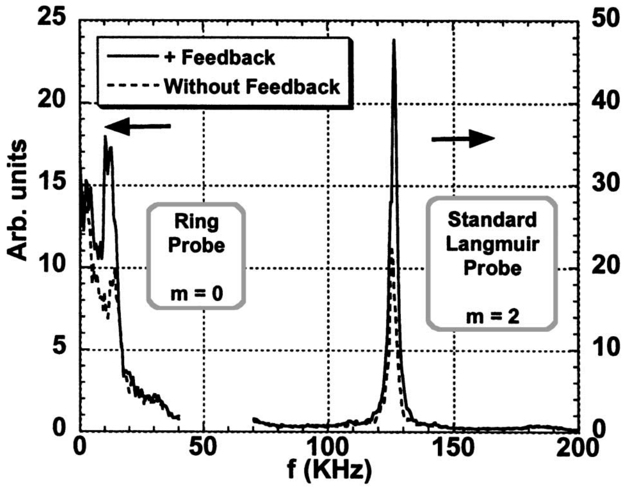

FIG. 5. The spectra from ring and standard Langmuir probes with and without feedback.

the sensitivity of detection of the very low level of IA, we use a ring Langmuir probe, which spatially filters out both the $m = 1$ and $m = 2$ modes and responds only to the $m = 0$, IA mode. This ring probe has a radius of 1.6 cm and wire diameter of 0.2 mm and is placed coaxial with the plasma column. The spectrum of the ion saturation current signal ($m = 0$) from the ring probe at low frequencies (0–40 kHz) and that from the standard Langmuir probe ($m = 2$) at higher frequency (70–200 kHz) are shown in Fig. 5. It is clear that with feedback enhancement of the ITG mode, the IA mode amplitude increases, demonstrating mode coupling between the two.

Based on the above experimental results, we now present a new paradigm for ion transport. We start with Kadomtsev mixing length scaling of transport

$$\chi_\perp \sim \gamma_d/k_\perp^2 \sim k_\parallel C_s/k_\perp^2 \sim A_i^{-1/2} \qquad (3)$$

as a rough guide. Here we have used the decorrelation frequency γ_d instead of the commonly used linear growth rate or the net growth rate. For the decorrelation frequency γ_d, we chose the ion acoustic mode damping, accessed via nonlinear mode coupling described above. Ion acoustic modes are highly damped in CLM plasmas (with $T_i \geq T_e$) with damping rate $\gamma_d \sim k_\parallel c_s \sim A_i^{-1/2}$. Furthermore, as $k_\perp$ is independent of ion mass in the CLM, as only very long wavelength modes with $k_\perp \rho_s \ll 1$ are observed, we obtain an inverse gyro-Bohm scaling in Eq. (3). It is now conjectured that the above basic physics scenario may be valid for tokamaks also; when the profile variation of $\omega_T^*(r)$ is considered to yield nonlocal radial harmonics, parallel ion dynamics is retained to yield transit ion resonance and damped ion acoustic modes, and only very long wavelength modes are considered important for transport as stated above. With these inclusions, the gyrokinetic code of Lee and Santoro and others may reveal the same physics basis as our proposed model.

One of the authors (A. K. S.) acknowledges fruitful discussions with Ron Waltz, Wendell Horton, and Willie Lee. This research was supported by U.S. Department of Energy Grant No. DE-FG02-98ER-54464.

[1] M. Bessenrodt-Weberpals *et al.*, Nucl. Fusion **33**, 1205 (1993).
[2] B. Coppi *et al.*, Plasma Phys. Controlled Nucl. Fusion Res. **2**, 413 (1991).
[3] B. D. Scott, Phys. Fluids B **4**, 2468 (1992).
[4] R. E. Waltz *et al.*, Phys. Plasmas **4**, 2482 (1997).
[5] D. R. Ernst *et al.*, Phys. Rev. Lett. **81**, 2454 (1998).
[6] V. Sokolov and A. K. Sen, Phys. Rev. Lett. **89**, 095001 (2002).
[7] W.W. Lee and R. A. Santoro, Phys. Plasmas **4**, 169 (1997).
[8] T. H. Dupree, Phys. Fluids **11**, 2680 (1968).
[9] R. Scarmozzino, A. K. Sen, and G. A. Navratil, Phys. Rev. Lett. **57**, 1729 (1986).
[10] A. B. Plaut, A. K. Sen, G. A. Navratil, and R. Scarmozzino, Phys. Fluids B **2**, 293 (1989).
[11] P. Tham and A. K. Sen, Phys. Plasmas **1**, 3577 (1994).
[12] W. Horton, Rev. Mod. Phys. **71**, 735 (1999).
[13] A. K. Sen, V. Reva, and K. Avinash, Phys. Plasmas **8**, 4772 (2001).
[14] Y. C. Kim and E. J. Powers, IEEE Trans. Plasma Sci. **PS-7**, 120 (1979).
[15] S. E. Parker and A. K. Sen, Phys. Plasmas **9**, 3440 (2002).